Graph Characteristics from the Schrödinger Operator

Pablo Suau[1], Edwin R. Hancock[2], and Francisco Escolano[1]

[1] Mobile Vision Research Lab, University of Alicante, Spain
{pablo,sco}@dccia.ua.es
[2] Department of Computer Science, University of York, UK
edwin.hancock@york.ac.uk

Abstract. In this paper, we show how the Schrödinger operator may be applied to the problem of graph characterization. The motivation is the similarity of the Schrödinger equation to the heat difussion equation, and the fact that the heat kernel has been used in the past for graph characterization. Our hypothesis is that due to the quantum nature of the Schrödinger operator, it may be capable of providing richer sources of information than the heat kernel. Specifically the possibility of complex amplitudes with both negative and positive components, allows quantum interferences which strongly reflect symmetry patterns in graph structure. We propose a graph characterization based on the Fourier analysis of the quantum equivalent of the heat flow trace. Our experiments demonstrate that this new method can be succesfully applied to characterize different types of graph structures.

Keywords: graph characterization, heat flow, Schrödinger equation, quantum walks.

1 Introduction

The analysis of graph and network topology is widely used in fields including computer vision, biology, data mining and linguistics. In all these areas, effective methods for characterizing or distinguishing different graph structures are essential, and as a result, many approaches to the graph characterization problem have been proposed, including algorithms based on random walks [1], the Ihara zera function [2] or the spectral radius [3]. Another family of graph characterization technique, introduced by Escolano *et al.* [4], can be derived from the analysis of the heat flow. Heat flow accounts for information transfer between nodes of a graph and it is determined by the heat kernel [5], and this in turn is the solution of the heat difussion equation.

Mathematically, the heat diffussion equation is similar to Schrödinger equation, which characterizes the dynamics of a particle in a quantum system [6]. However, similarities are superficial since both underlying physics and the dynamics induced by the Schrödinger equation are different to those induced by the heat difussion equation. In this paper we demonstrate that the solution of the

W.G. Kropatsch et al. (Eds.): GbRPR 2013, LNCS 7877, pp. 172–181, 2013.

Schrödinger equation, i.e. the Schrödinger operator, may provide a useful tool for characterizing graph structure. The quantum nature of the Schrödinger operator gives rise to several interesting non-classical effects including quantum interferences produced by the negative components of the complex amplitudes arising from the solution of Schrödinger equation. Moreover, interferences proved to be useful in several applications, e.g. detection of symmetric motifs in graphs via continuous-time quantum walks [7] or graph embedding by means of quantum commute times [8]. Furthermore, the quantum nature of the amplitude must also be taken into account when designing new methods and algorithms based on the Schrödinger operator. For instance, dynamic systems based on the Schrödinger operator, e.g. continuous-time quantum walks, are non-ergodic. In this paper, we propose a new graph characterization method that exploits features due to non-ergodicity.

The remainder of this paper is structured as follows. In Section 2 we summarize the concept of heat flow for graph characterization. In Section 3 the Schrödinger operator is introduced. The main contributions of this paper are presented in Section 4, in which we formally analyze the Schrödinger operator and propose a new graph characterization technique based on an equivalent of the heat flow. Then, in Section 5, we show some experimental results. Finally we draw some conclusions and point out ways in which this work can be further extended.

2 Heat Flow

Let $G = (V, E)$ be an undirected graph where V is its set of nodes and $E \subseteq V \times V$ is its set of edges. The Laplacian matrix $L = D - A$ is constructed from the $|V| \times |V|$ adjacency matrix A, in which the element $A(u, v) = 1$ if $(u, v) \in E$ and 0 otherwise, where the elements of the diagonal $|V| \times |V|$ degree matrix are $D(u, u) = \sum_{v \in V} A(u, v)$. The $|V| \times |V|$ heat kernel matrix K_t is the fundamental solution of the heat equation

$$\frac{\partial K_t}{\partial t} = -LK_t, \tag{1}$$

and depends on the Laplacian matrix L and time t. It describes how information flows across the edges of a graph with time, and its solution is $K_t = e^{-Lt}$.

The heat kernel K_t is a doubly stochastic matrix. Double stochasticity implies that diffusion conserves heat. In [4], a graph is characterized from the constraints it imposes to heat diffusion due to its structure. This characterization is based on the normalized instantaneous flow $F_t(G)$ of graph G, that accounts the edge-normalized heat flowing through the graph at a given instant t, and it is defined as:

$$F_t(G) = \frac{2|E|}{n} \sum_{i=1}^{n} \sum_{j \neq i} A(i, j) \left(\sum_{k=1}^{n} \phi_k(i) \phi_k(j) e^{-\lambda_k t} \right). \tag{2}$$

A more compact definition of the edge-normalized instantaneous flow is $F_t(G) = (2|E|/n)A : K_t$, where $X : Z = trace(XZ^T)$ is the Frobenius inner product. The heat flow trace describing the graph is constructed by computing Eq. 2 on the interval $[0, t_{max}]$.

3 Heat Kernel vs. Schrödinger Operator

The Schrödinger equation describes how the complex state vector $|\psi_t\rangle \in \mathbb{C}^{|V|}$ of a continuous-time quantum walk varies with time [9]:

$$\frac{\partial|\psi_t\rangle}{\partial t} = -iL|\psi_t\rangle. \tag{3}$$

Given an initial state $|\psi_0\rangle$ the latter equation can be solved to give $|\psi_t\rangle = \Psi_t|\psi_0\rangle$, where $\Psi_t = e^{-iLt}$ is a complex $|V| \times |V|$ unitary matrix. In this paper we refer to Ψ_t as the *Schrödinger operator*. Our attention in this paper will be focused on the operator itself and not on the quantum walk process. As can be seen, Eq. 3 is similar to Eq. 1. However, the physical dynamics induced by the Schrödinger equation are totally different, due to the existence of oscillations and interferences.

In this section we address the question of whether the Schrödinger operator may be used to characterize the structure of a graph. Empirical analysis on different graph structures shows that both the heat kernel and the Schrödinger operator evolve with time in a manner which strongly depends on graph structure. [1] However, the underlying physics and the dynamics are different (see Fig. 1). In the case of heat flow heat diffuses between nodes through the edges, eventually creating transitive links (energy exchanges between nodes that are not directly connected by an edge), until reaching a stationary energy equilibrium state. The Schrödinger operator yields a faster energy distribution through the system (e.g. for a 100 nodes line graph, it takes $t = 50$ time steps for the Schrödinger operator to reach every possible position on the graph, taking more than twice this time in the case of the heat kernel). Moreover, due to negativecomponents of the complex amplitudes, interferences are created, producing energy waves. The main difference is that the Schrödinger operator never reaches an equilibrium state. In other words, it is non-ergodic. Graph connectivity imposes constraints on the distribution of energy. In the case of the heat kernel, a higher number of energy distribution constraints implies the creation of more transitive links with time [4]. This is also true in the case of the Schrödinger operator, for which lower frequency and more symmetrical energy distribution patterns are also observed.

3.1 Analysis of the Schrödinger Operator

Further formal analysis of the Schrödinger operator supports the empirical evidence stated above. We first consider the Schrödinger operator when t tends to zero. Its Taylor expansion is given by:

$$\Psi t = e^{-iLt} = \cos Lt - i \sin Lt = I_{|V|} - iLt - \frac{t^2}{2!}L^2 + i\frac{t^3}{3!}L^3 + \frac{t^4}{4!}L^4 \cdots, \tag{4}$$

[1] Videos showing the evolution of both heat kernel and Schrödinger operator are available at `http://www.dccia.ua.es/~pablo/downloads/schrodinger_operator.zip`

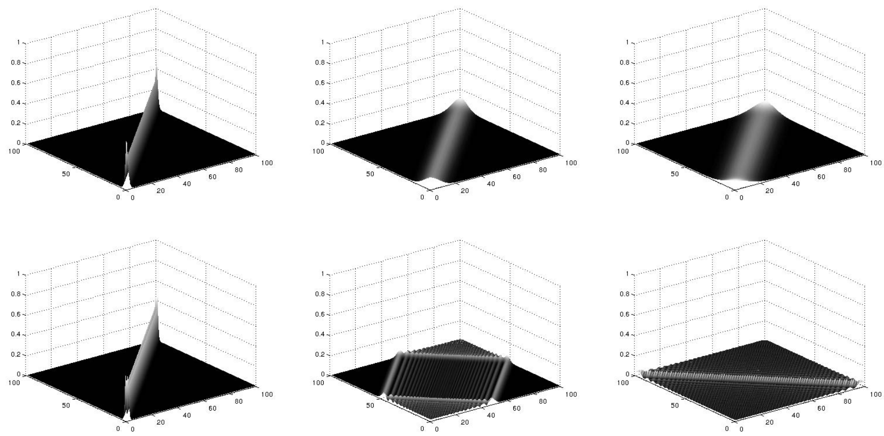

Fig. 1. Evolution of the keat kernel (top) and the Schrödinger operator (bottom) with time ($t = 1, 25$ and 50) for a 100 node line graph

where $I_{|V|}$ is the $|V| \times |V|$ identity matrix. Hence

$$\lim_{t \to 0} \Psi_t \approx I_{|V|} - iLt, \tag{5}$$

where $\Psi_t = K_t$ when $t = 0$. At this time instant every node conserves its energy (as in the case of the Heat Kernel). The role of the identity matrix is to make the Schrödinger operator unitary. Due to the $-iLt$ term, it can be seen that energy spreads as a wave even for t values close to zero. Thus, the Schrödinger operator causes energy to distribute in a waveform from the initial time instant.

In order to explore the ergodicity of the Schrödinger operator we consider both its spectral decomposition and that of the heat kernel:

$$K_t = \sum_{p=1}^{n} e^{-t\lambda_p} \phi_p \phi_p^T \text{ and} \tag{6}$$

$$\Psi_t = \sum_{p=1}^{n} e^{-it\lambda_p} \phi_p \phi_p^T, \tag{7}$$

where λ_p is the p-th eigenvalue of the Laplacian L and ϕ_p its corresponding eigenvector.

The spectral decomposition of the heat kernel demonstrate that it is dominated by the lowest eigenvalues, due to the fact that $e^{-t\lambda_p}$ tends to zero as t tends to infinity. However, $e^{-it\lambda_p}$ is indefinite when t tends to infinity. Thus, there are two importante differences with the heat kernel. Firstly, the Schrödinger operator never converges (it is non-ergodic), and secondly, it is not dominated by any particular eigenvalue (i.e. there is more dependence on global graph structure as t tends to infinity).

Finally, we can compare the Euler equation based Schrödinger operator Ψ_t with the wave equation formula

$$\psi = \upsilon e^{i(kx - wt + \epsilon)}, \tag{8}$$

where υ is the amplitude, ϵ is the initial phase, k is the wavenumber, and w is the angular frequency. Schrödinger operator can be interpreted as a wave with $\upsilon = 1$, $k = \epsilon = 0$ and $w = L$. In fact, Eq. 7 expresses the Schrödinger operator as a linear combination of $p = 1 \cdots n$ waves with different frequencies λ_p.

3.2 The Quantum Energy Flow

As stated in Section 2 the heat flow characterizes a graph by means of a trace that accounts for the information flowing on the graph with time. Due to the similarity between the heat diffusion and the Schrödinger equations, we could define quantum energy flow (QEF) as

$$Q_t(G) = A : \Psi_t, \tag{9}$$

and the quantum energy trace (the equivalent of heat flow) as the evolution of Q_t with time. It must be noted that the hamiltonian of the quantum system defined by Ψ_t is given by the graph laplacian L. The adjacency matrix A in Eq. 9 causes the QEF to only account for the energy distributing through edges. In Fig. 2 we compare the heat flow and the QEF traces for two different types of graph. In [4], graph structure is characterized by the heat flow's phase transition point (PTP). The overall information transmited in the system increases until reaching a PTP, and then decreases until convergence. This is ilustrated inf Fig. 2 (left). A PTP based caractherization can not be applied in the case of the Schrödinger operator, due to its non-ergodicity and the existence of several PTPs. However, we observe again a difference in phase transition frequency depending on the structure of the graph.

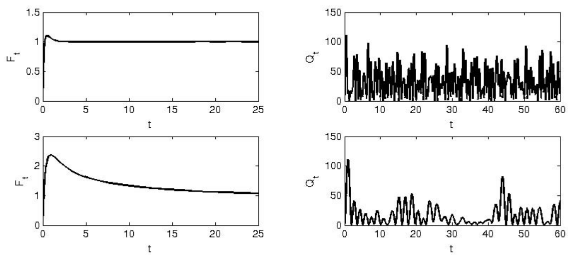

Fig. 2. Heat flow (left) and QEF (right) for two different 10 node graphs: a random graph (top) and a line graph (bottom). In both cases, the x axis represents time.

3.3 Frequency Domain Analysis of the Schrödinger Operator

The results and analysis above suggest a correlation between graph structure and both the Schrödinger operator and the QEF frequency patterns. We therefore propose a graph characterization based on the QEF in the frequency domain. In order to obtain this characterization, we consider the QEF as a non-periodic signal: we select a time interval $[0, T]$ and we apply the Fast Fourier Transform to the QEF. We refer to this representation as the *frequency domain trace*. The frequency domain trace for the graphs in Fig. 2 can be seen in Fig. 3. The first conclusion from these plots is that the more complex graphs are characterized by the presence of higher frequencies.

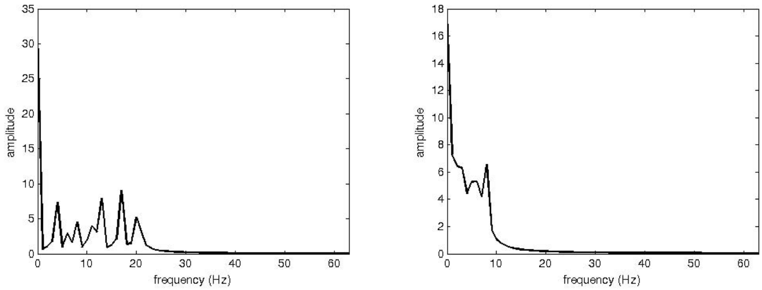

Fig. 3. Frequency domain trace obtained from the quantum energy flow of the random graph (left) and the line graph (right) in Fig. 2

However, this representation depends on graph size. Fig. 4 (left) shows the frequency domain trace for four differently sized line graphs. This plot demonstrates that the maximum spectral amplitude is proportional to the graph size. In order to compare arbitrarely sized graphs we apply a simple frequency domain trace normalization based on its maximum amplitude. The result of this normalization can be seen in Fig. 4 (right).

During our experiments we will represent graphs by means of a *cumulative frequency domain trace*, obtained by accumulating the normalized amplitudes from lower to higher frequencies of their corresponding frequency domain traces. In Fig. 5 we compare the cumulative frequency domain trace obtained from five graphs and their corresponding heat flows. In the case of the cumulative frequency domain trace, the area under the curve provides a good estimate of graph complexity. Simpler graphs yield larger areas. The PTPs of the corresponding heat flow traces also provide a good complexity estimate. In this case, the PTP for simple graphs is reached later in time. However, in this particular example, the heat flow trace estimates the complexity of the line graph to be lower than that of the circle graph. That is not the case of the cumulative frequency domain trace, for which the complexity of the line graph is higher.

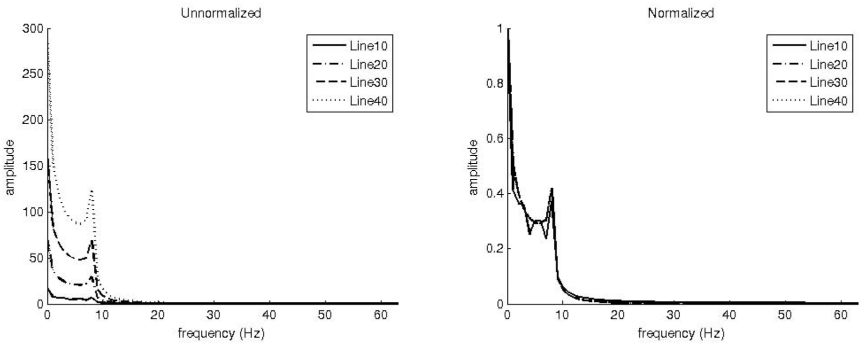

Fig. 4. Unnormalized (left) and normalized (right) frequency domain traces for four different size line graphs (10, 20, 30 and 40 nodes)

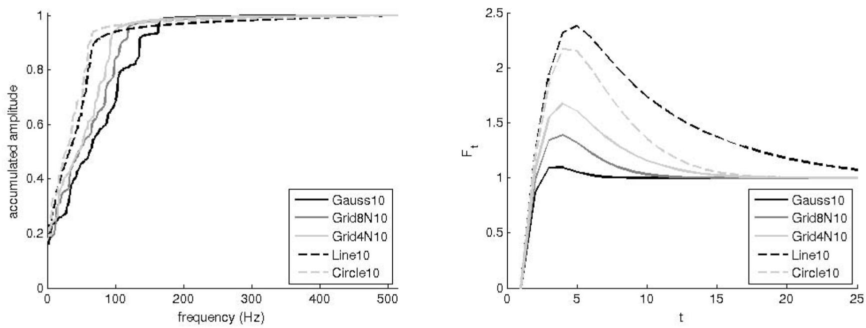

Fig. 5. Cumulative frequency domain traces (left) and heat flow (right) for five simple 10 node graphs: a random graph (Gauss10), a 8-connected 2x5 grid (Grid8N10), a 4-connected 2x5 grid (Grid4N10), a line graph (Line10) and a circular graph (Circle10)

4 Experimental Results

4.1 Noise Sensitivity

The aim of this first experiment is to show the sensitivity of frequency domain traces to graph noise. We first constructed a base 400 nodes random graph by means of the Erdös-Rényi model [10]. We then compared the frequency domain trace of the base graph to those obtained after applying random edit operations on it. In this experiment we only applied edge removal operations, and thus, in each iteration, we remove a random edge from the base graph and we compute the Euclidean trace between the unnormalized traces. The results are shown in Fig. 6. Four experiments were performed, using four different time intervals $[0..T]$ to construct the frequency domain traces.

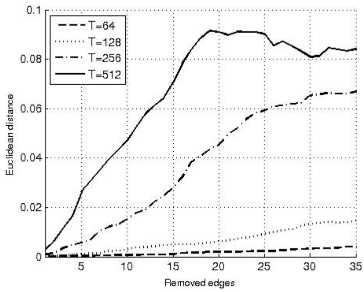

Fig. 6. Results of the noise sensitivity experiment. Number of edit operations (edge removals) versus distance between edited graph's frequency domain trace and base graph's one, for four different T values.

From Fig. 6, it is clear that the final trace is not strongly affected by small disturbances. For larger time intervals there appears to be a significant sensitivity to noise. However, difference between traces is still low. The remainder of the experiments in this paper are conducted after setting $T = 1024$.

4.2 Graph Characterization

In order to test the discriminative power of our characterization we constructed a dataset of synthetic graphs. The dataset consists of three groups of 32 graphs, each group characterized by a different graph structure. All of the graphs in the dataset have 90 nodes. The graphs in the first group are random graphs constructed using the Erdös-Rényi [10] model, in which each pair of nodes is linked by an edge with probability given by p. In our experiments we set $p = 0.1$. The graphs in the second group belong to the category of scale free graphs (i.e. graphs for which its degree distribution follows a power law), and were constructed using the Barabási and Albert's model [11].In this model we have set $m_0 = 5$ for the initial size of the graphs and $m = 2$ for the number of links to add during each iteration, following the addition of a node. Finally, the graphs in the third group correspond to small world graphs (i.e. graphs in which most nodes are not neighbours of each other, but in which average path length between a graph pair of nodes is small). These small world graphs are generated by means of the Watts and Strogatz algorithm [12]. In this case we set the mean degree value to $K = 10$ and the rewiring probability to $p = 0.2$.

A cumulative frequency domain trace was computed for all graphs in the set, and the results are shown in Fig. 7. The first conclusion of our experiment is that these traces clearly discriminate between different graph structures. This conclusion is supported by a Multidimensional Scaling analysis (MDS) of the traces (also shown in Fig. 7). The aim of MDS is to apply dimensionality reduction on data while preserving relative distances between patterns. If we project the traces onto a 2D space, the graphs in the three groups are clearly split into three different clusters with high intra-cluster homogeneity and high-inter cluster separability.

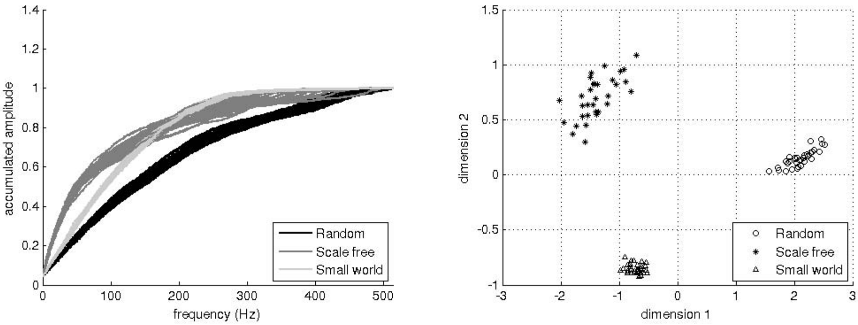

Fig. 7. Characterization of synthetic graphs. Left: cumulative frequency domain traces. Right: MDS results.

In Fig. 7 we explore the relationship between frequency and structure. The frequency spectrum of random graphs is characterized by higher amplitudes at high frequencies. In the case of small world graphs, the predominant frequencies are in the middle part of the spectrum. Scale free graphs are characterized by higher amplitudes at lower frequencies. These results suggest that the structure of random graphs is more complex in the sense that it imposes more constraints to the distribution of energy on the graph. As a consequence, energy waves exhibit higher frequency as they propagate. Scale free and small world graphs impose less restrictions on the distribution of energy through the graph, and are associated with lower frequency patterns.

5 Conclusions and Future Work

Heat flow, based on the heat kernel, has been succesfully used to characterize graph structure. The aim of the present paper was to answer the question of whether the Schrödinger operator (the solution to the Schrödinger equation) can be used also to characterize graph structure. After analyzing energy distribution through the graph based on the Schrödinger operator, we introduced a new characterization method based on the analysis in the frequency domain. Our experiments show that the *cumulative frequency domain trace* is a useful tool for graph analysis, that is not sensitive to small changes in graph structure.

However, based on these promising preliminary results, further in depth analysis is required. Firstly, and similarly to heat flow, the cumulative frequency domain trace does not provide us with a quantitative measure to directly compare graph structures. A first step in this direction could be to apply this trace as part of the thermodynamic depth complexity measurement framework, in order to obtain a numerical representation of graph structure [4][13]. Secondly, during our analysis of the Schrödinger operator we detected the presence of symmetric energy distribtuion patterns on the graph. We could analyze how this symmetry depends on graph structure and whether the results of this analysis are related to previous work on symmetry detection based on quantum walks [7]. Finally, it would be interesting to relate the Schrödinger operator and the cumulative frequency domain trace representation to the structure of complex network systems such as social or biological networks.

References

1. Aziz, F., Wilson, R.C., Hancock, E.R.: Graph Characterization via Backtrackless Paths. In: Pelillo, M., Hancock, E.R. (eds.) SIMBAD 2011. LNCS, vol. 7005, pp. 149–162. Springer, Heidelberg (2011)
2. Peng, R., Wilson, R., Hancock, E.: Graph Characterization vi Ihara Coefficients. IEEE Transactions on Neural Networks 22(2), 233–245 (2011)
3. Das, K.C.: Extremal Graph Characterization from the Bounds of the Spectral Radius of Weighted Graphs. Applied Mathematics and Computation 217(18), 7420–7426 (2011)
4. Escolano, F., Hancock, E., Lozano, M.A.: Heat Diffusion: Thermodynamic Depth Complexity of Networks. Physical Review E 85(3), 036206(15) (2012)
5. Xiao, B., Hancock, E., Wilson, R.: Graph Characteristics from the Heat Kernel Trace. Pattern Reognition 42(11), 2589–2606 (2009)
6. Aubry, M., Schlickewei, U., Cremers, D.: The Wave Kernel Signature: A Quantum Mechanical Approach To Shape Analysis. In: IEEE International Conference on Computer Vision (ICCV), Workshop on Dynamic Shape Capture and Analysis (4DMOD) (2011)
7. Rossi, L., Torsello, A., Hancock, E.R.: Approximate Axial Symmetries from Continuous Time Quantum Walks. In: Gimel'farb, G., Hancock, E., Imiya, A., Kuijper, A., Kudo, M., Omachi, S., Windeatt, T., Yamada, K. (eds.) SSPR & SPR 2012. LNCS, vol. 7626, pp. 144–152. Springer, Heidelberg (2012)
8. Emms, D., Wilson, R.C., Hancock, E.R.: Graph Embedding Using Quantum Commute Times. In: Escolano, F., Vento, M. (eds.) GbRPR. LNCS, vol. 4538, pp. 371–382. Springer, Heidelberg (2007)
9. Farhi, E., Gutmann, S.: Quantum Computation and Decision Trees. Physical Review A 58, 915–928 (1998)
10. Erdös, P., Rényi, A.: On Random Graphs. I. Publicationes Mathematicae 6, 290–297 (1959)
11. Barabási, A.L., Albert, R.: Emergence of Scaling in Random Networks. Science 286(5439), 509–512 (1999)
12. Watts, D.J., Strogatz, S.H.: Collective Dynamics of 'Small-World' Networks. Nature 393(6684), 440–442 (1998)
13. Han, L., Escolano, F., Hancock, E., Wilson, R.: Graph Characterizations From Von Neumann Entropy. Pattern Recognition Letters 33(15), 1958–1967 (2012)